Phenazines as chemosensors of solution analytes and as sensitizers in organic photovoltaics

Subhadeep Banerjee

Birla Institute of Technology and Science-Pilani, K. K. Birla Goa Campus
NH-17B By-Pass, Zuarinagar, Goa-403726, India
E-mail: subhadeepb@goa.bits-pilani.ac.in

DOI: http://dx.doi.org/10.3998/ark.5550190.p009.347

Abstract
This review aims to highlight phenazines as photoactive molecules with applications arising from its unique optical properties. Synthesis and optical spectra of a number of phenazines possessing absorption and emission signals in the visible range was reported. Applications described included sensing of cations, anions and as sensitizers in organic photovoltaics.

Keywords: Phenazines, UV-visible absorption, fluorescence, chemosensing, organic photovoltaics

Table of Contents

1. Introduction

The planar structure of phenazine with a heterocyclic pyrazine core and a fully conjugated aromatic π-system imparts to it special optical and redox properties. The optical properties render it useful for applications in molecular imaging as fluorescent tracers and stains for sub-cellular components and biological events. Some of the well-known fluorescent stains (Figure 1) for histological purposes possess a phenazine moiety as the core structure; eg.

safranine **1** which is used as a counterstain in some staining protocols,[1] neutral red **2** used for staining lysosomes,[2] janus green B **3** a basic dye and a vital histological stain[3] and the intensely luminescent 2,3-diaminophenazine **4**, useful for fluorimetric determination of laccase activity.[4] All these fluorescent phenazines have their absorption and emission spectra in the physiologically relevant region of 400-700 nm. On account of its planarity phenazine also serves as a strong DNA-intercalator thereby exhibiting potent anti-tumor and anti-microbial activity. Example include ligands based on dipyrido[3,2-*a*: 2',3'-*c*]phenazine (DPPZ) that have been used in preparing transition metal-phenazine coordination complexes **5**, which were further studied for their DNA intercalative properties.[5] In course of DNA-intercalation, phenazine absorption and fluorescence could vary substantially depending on the type of nucleotides present in a binding site. Fluorescent phenazines have also been used as selective cations[6] and anion binding agents[7] due to their optical spectral alterations and colorimetric changes upon analyte binding, whereby the latter would aid in the 'naked-eye' detection. These compounds are capable of intramolecular charge transfer (ICT), modulation of which by the analyte binding leads to the signal amplification and or ratiometric spectral shifts.

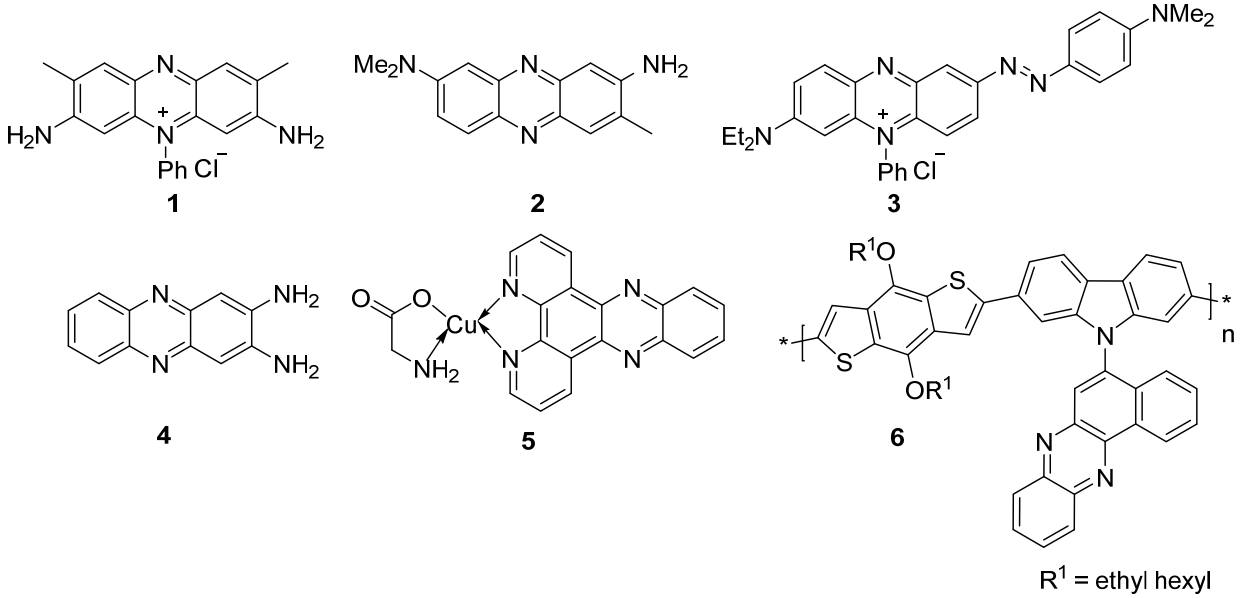

Figure 1. Examples of phenazine based dyes, metal complexes and polymers.

Highly electron-rich and redox-active molecules such as phenazines could be useful for preparation of organic smart materials featuring donor-π-acceptor architecture.[8] These are important for imparting red-light emissions for applications in organic light emitting devices (OLED),[9] as semiconductors in thin film transistors (TFT)[10] and as sensitizers in dye-sensitized solar cells (DSSCs).[11] Existence of a donor-acceptor (D-A) alternating structure has been proved to be an effective way to reduce bandgap energies of conjugated polymers. Since the phenazine core consists of the electron withdrawing pyrazine ring which can be a good charge acceptor,

phenazine-acene (PA) based polymers such as compound **6** (Figure 1) have been used for construction of low band gap organic materials.[12]

While the synthesis, biological activity and huge natural products database on phenazines has been extensively reviewed,[13] there is also scope for reviewing the phenazines as a distinct class of photoactive heteroaromatic acenes, whose unique photophysical properties have rendered them useful as fluorescent dyes, chemosensors and as redox-active building blocks of organic materials. A review on heteroaromatic fluorescent dyes was published by Nau *et. al* in 2011[14] highlighting a number of well-known molecules and their supramolecular complexes with macrocycles. These include xanthenes, coumarins, squarines, and other polycyclic aromatic dyes bearing complex structures. The review deals with changes to their photophysical properties upon complexation with hosts such as cylcodextrin, cucurbit[*n*]turils. The structural simplicity and easy synthesis of the phenazine moiety in comparison to the other dyes mentioned does make it a good candidate for possible exploration for further modifications towards creation of a library of fluorescent phenazine based molecules. Thus, it is important to review the progress achieved so far in the field of synthesis and applications of photoactive phenazines. The, the aim of this review is to cover the preparation of photoactive phenazines, their optical spectral elucidation, report on the analysis of their molecular orbitals and highlight how phenazines have been used in solution analyte sensing and in organic photovoltaics.

2. Applications Based on Photophysical Properties of Phenazines

2.1 Structure-optical property correlations of phenazine-based dyes

Theoretical studies have been carried out on the phenazines in order to explain effect of substituents on its optical spectra and nature of electron distribution. These studies elucidate the picture of the frontier molecular orbitals and thus are important for designing of phenazine based chemosensors and chemodosimeters. Appropriate placement of electron donor groups on the phenazine periphery in conjugation with its electron accepting pyrazine core would promote ICT giving rise to red-shifted optical spectra. This was found to be true for a number of examples. Robbins *et. al* have reported through theoretical studies on 2,3-dialkoxy phenazines that attaching halogen groups at the 7,8-positions of the phenazine core could reduce its lowest unoccupied molecular orbital (LUMO) energy level considerably. In addition, the attachment of long chain alkoxy groups in the 2,3-positions of the heteroaromatic core could act as strong electron donating groups increasing the extent of intramolecular charge transfer (ICT) and also help enhance solubility in organic solvents.[15] A few examples of phenazines with halogen substituents at the 7,8-positions were prepared[16] (Scheme 1).

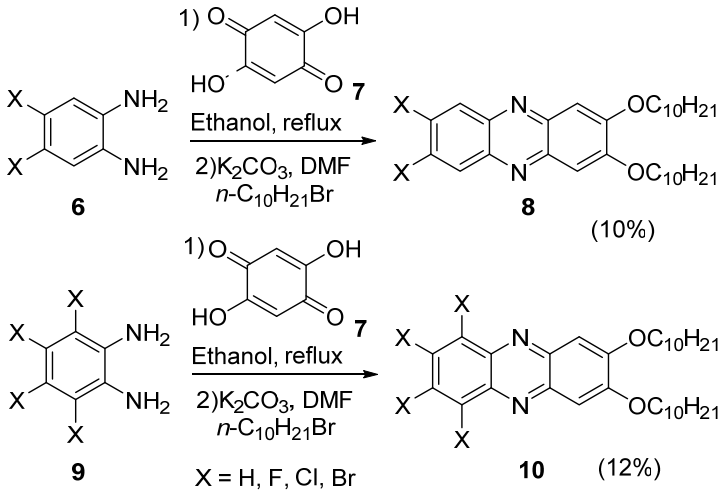

Scheme 1. Synthesis of halogen substituted dialkoxy phenazines.

The λ_{max} for compound **8** in the UV-visible absorption spectrum (Figure 2A) was red-shifted from 390 nm to 405 nm on proceeding from substituent H to F to Cl to Br. Within one type of halogen a further lowering of the LUMO energy was observed theoretically and experimentally when the number of halogen substituents was increased from two to four (Scheme 1 compound **10**). If the dichloro-substituted phenazine **8Cl** possessed a λ_{max} at 400 nm, its corresponding tetra-substituted derivative **10Cl** was red-shifted to 410 nm (Figure 2B). This was again attributable to greater extent of LUMO stabilization upon addition of higher numbers of electron withdrawing halogen atoms to the phenazine core.[15]

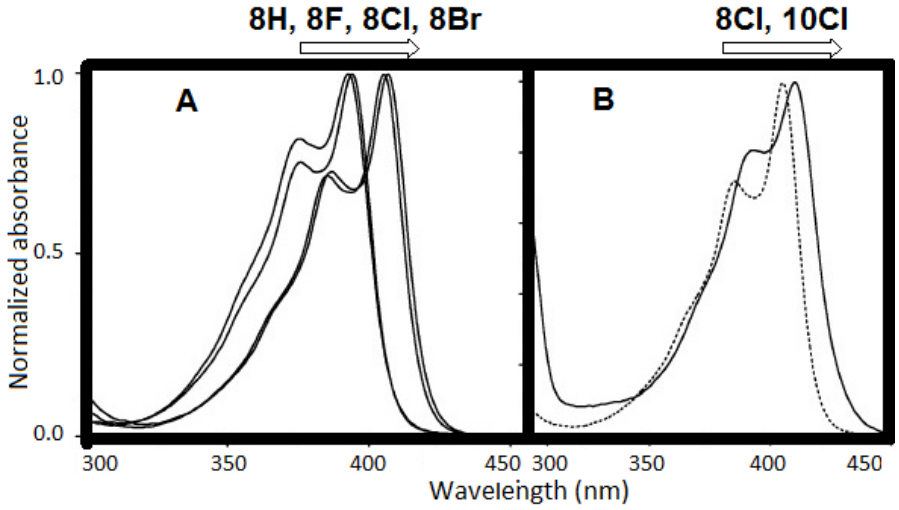

Figure 2. UV-visible spectral comparisons of (A) **8H**, **8F**, **8Cl**, **8Br** and (B) **8Cl**, **10Cl**; adapted from reference 15.

Theoretical and experimental analysis of the optical properties of another analogous phenazine 2,3-diaminophenazine **4** were also performed. 2,3-diaminophenazine (DAP) is a planar electron rich phenazine possessing strong luminescence in polar organic solvents as also in aqueous buffer solutions, notably when embedded inside a micelle structure.[17] Through density functional theory (DFT) calculations Sylvestre et al. have performed vibration analysis and natural bond orbital analysis of DAP.[18] Vibrational analysis indicates simultaneous existence of the C–C stretching mode for both its IR and Raman spectra thereby allowing delocalization of charge from electron donating amino groups to the phenazine ring. Additionally, the theoretically computed HOMO and LUMO energy gap closely matches with the observed λ_{max} peak at 419 nm in its UV-visible absorption spectrum (Figure 2A). Molecular electrostatic potential (MEP) analysis also revealed the highest degree of negative charge accumulation to be on the pyrazine nitrogen atoms (Figure 2B).[18] Expectedly the 2,3-diamino group in **4** being a stronger electron donor than the 2,3-dialkoxy groups in **8** and **10** (Scheme 1) as reflected in the *para*-Hammett constants (σ_p values for -NH_2 is -0.66 and for –OEt is -0.25),[19] the extent of ICT in **4** is higher than that in **8** and **10** which is why the corresponding λ_{max} is modestly red-shifted (419 nm over 410 nm).

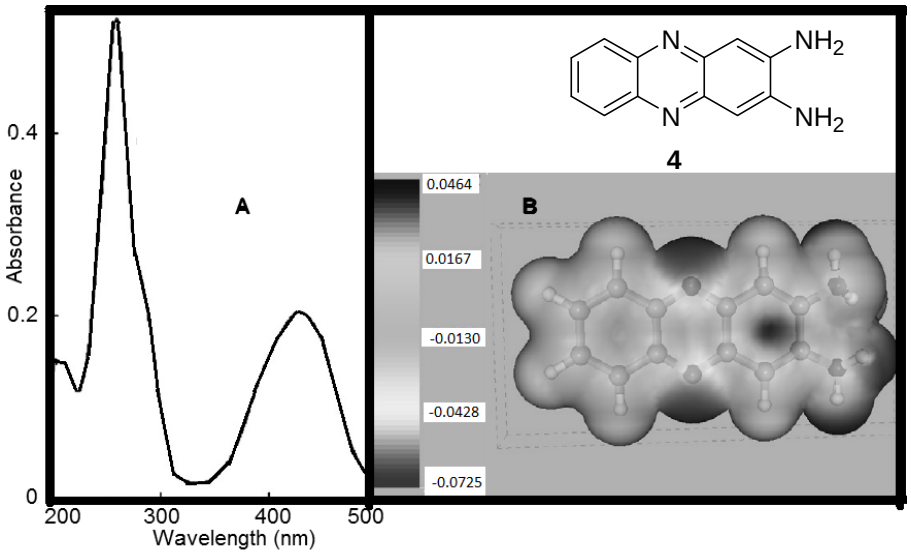

Figure 3. (A) UV-visible absorption spectrum of **4** in ethanol and (B) molecular electrostatic potential diagram of **4** indicating regions of high electron density in dark grey and low electron density in light grey; adapted from reference 18.

A pH sensitive imidazole-fused phenazine **11** was reported by Ryazanova *et. al*[20] capable of exhibiting reversible optical spectral changes upon pH alterations between pH ranges from 0-14. The UV-visible spectral λ_{max} for **11** was centered on 440 nm under neutral pH conditions for these examples while the simple unmodified phenazine peak was at 400 nm in neutral aqueous buffer solutions.[20] This difference could be attributed to a larger π-electron system due to fusion

of the imidazole ring with the phenazine nucleus. Under high pH conditions (~12) bathochromic shifting of the λ_{max} signal by about 60 nm was observed. The pka of **11** was spectrophotometrically determined to be 10.9. Hence, the observed red-shift was explained to originate from the deprotonation of the imidazole acidic hydrogen and further delocalization of the charge on the anionic nitrogen into the central phenazine core. This is also supported by the fact that if the imidazole acidic hydrogen is replaced by a sugar moiety the observed bathochromic spectral shift at alkaline pH (~12) disappears.[20] Phenazine UV-vis spectrum itself is unaffected by increasing pH of the medium. **11** exhibts a fluorescence emission in the biologically relevant region of 566 nm in aqueous buffer solutions of pH 6 and exhibit fluorescence turn-off behavior under strongly acidic pH.[20]

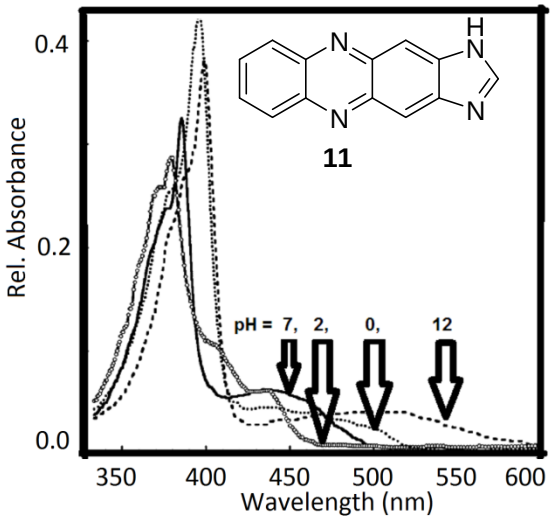

Figure 4. UV-visible absorption spectra of **11** in different buffer solutions of varying pH; adapted from reference 20.

Aminoperfluorophenazines as examples of push-pull phenazines were prepared by Matsui *et. al.* using a nucleophilic aromatic substitution reaction[21] as shown in Scheme 2 between an alkyl/aryl amine and the highly electron deficient perfluorophenazine (the latter prepared by electrochemical oxidation of fluoroaniline).[21]

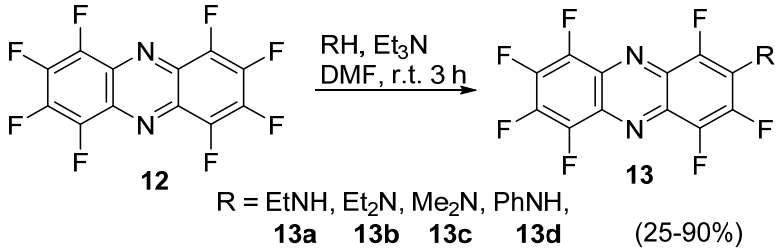

Scheme 2. Synthesis of 2-amino-1,3,4,6,7,8,9-heptafluorophenazine.

UV-vis spectra of phenazines and perfluorophenazines are similar (λ_{max} = 362 nm and 367 nm respectively in hexanes),[21] however the aminoperflurophenazines are more red-shifted (λ_{max} at 456 nm in hexanes for **13a**, σ_p values for -NHEt = -0.61[22]) (Figure 5). The UV-visible spectrum of compound **13a** exhibits positive solvatochromism and red-shifts by about 30 nm on proceeding from non-polar hexane to polar solvent ethanol. This observation could be explained by the increase in dipole moment of **13a** from the ground state to the excited state (5.32 and 9.19 D respectively) whereby the more polarized excited state is better stabilized in the more polar solvent. While phenazine itself in non-fluorescent and perfluorphenazine is weakly emissive, the intense fluorescence of the amino substituted phenazines was evident from their measured fluorescence quantum yield values that were in the range of 0.92-0.98. The emission spectra of the prepared compounds possessed signals in the range of 524-613 nm. The fluorescence spectrum of compound **13a** was also susceptible to positive solvatochromic changes, although the fluorescence intensity reduced drastically in more polar solvents.[21]

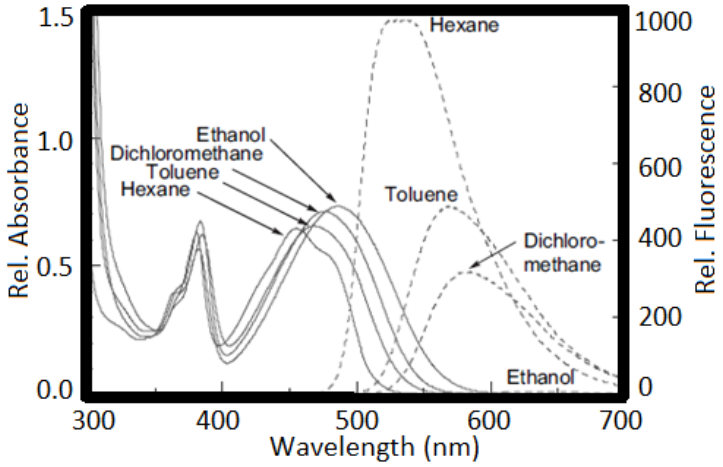

Figure 5. UV-visible and fluorescence spectrum of compound **13a** reflecting its solvatochromic behavior; adapted from reference 21.

Thomas *et. al.* have described the synthesis and photophysical characterization of some amine-substituted benzophenazines prepared from *o*-naphthoquinones and aromatic/aliphatic amines (Scheme 3).[23] The synthesis involves a Michael addition-oxidation reaction to generate the fully congujated aromatic intermediate **16** followed by a double condensation with *o*-phenylene diamine to yield the benzophenazines **17**.

These molecules exhibited broad absorption peaks around 450 nm in toluene (Figure 6). The origin of the absorption peaks were primarily due to benzophenazine localized π-π* transitions and a minor component arising from charge transfer between the amine and pyrazine segment, as revealed through by DFT computations on the electronic structure of the dyes. The absorption spectra were bathochromically shifted by ~100 nm upon addition of 10 fold equivalents of trifluoroacetic acid (Figure 6). The optical spectral shifting was also visible to the naked eye as a

colorimetric transition from yellow (neutral pH) to pink/purple color (acidic pH), fully reversible upon neutralization of the acid with added base.

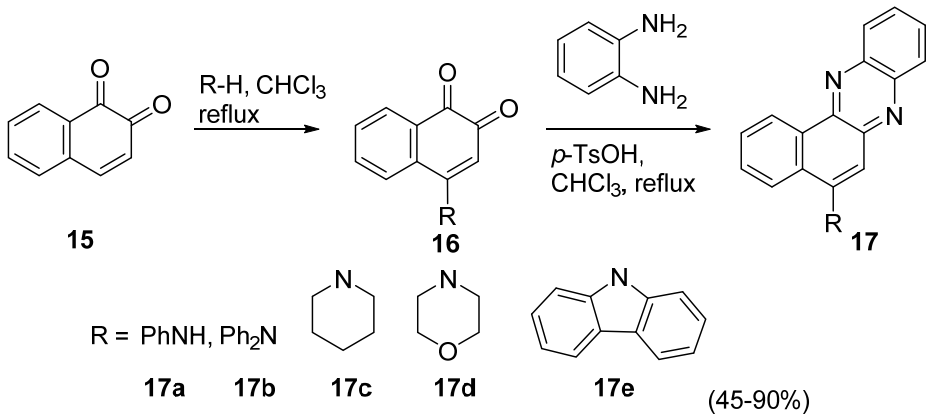

Scheme 3. Synthesis of 3-aminobenzo[a]phenazines.

This prominent red-shifting behavior was attributed to protonation at the pyrazine moiety of the phenazine rendering it a better charge acceptor and resultant LUMO stabilization, while the alkyl/aryl amine component functioned as a charge donor. Theoretical calculations also supported these findings whereby the HOMO was mostly delocalized between the amine moiety and its adjacent phenyl rings, while the LUMO was mostly concentrated in the quinoxalino moiety, with overlapping regions with the HOMO. Upon protonation there is a shifting of the HOMO towards the quinoxalino ring (depending upon the donor strength of the amine unit), which promotes further charge transfer and hence bathochromic shifting of the optical spectrum. The benzophenazines exhibited moderate intensity emission spectra (quantum yields Φ = 0.18-0.27) in the range of 504 to 543 nm in toluene. They also exhibited a positive solvatochromic shift upto 600 nm and decrease of emission intensity. Upon acidification the emission intensity is reduced. The redox properties of the compounds studied using cyclic voltametric methods indicated low oxidation potentials for derivatives bearing more electron donating aliphatic amino donor groups and lower reduction potentials for derivatives with arylamino substituents. This also pointed to the presence of a charge transfer mechanism from the amino donor to the pyrazine acceptor, the strength of which depended on the overall electron donating ability of the amine group.[23]

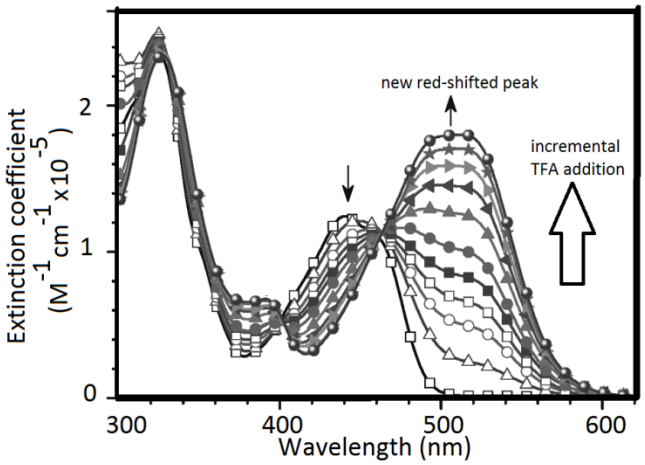

Figure 6. UV-visible spectrum of **17a** in toluene under neutral pH and after incremental addition of upto 10 fold equivalents of trifluoroacetic acid; adapted from reference 23.

A series of phenazine salens were synthesized through condensation reaction between 2,3-diaminophenazine and a number of 2-hydroxy-aryl aldehydes (Scheme 4).[24]

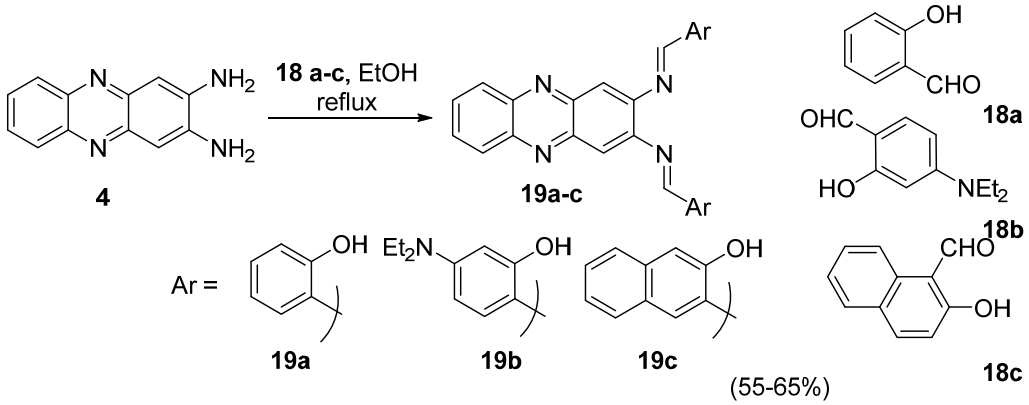

Scheme 4. Synthesis of phenazine salens.

The molecules exhibited strong absorption in the visible region and also moderate emission in the range of 500-550 nm with quantum yields Φ = 0.20 and 0.34 for **19** and **19b** respectively. The compound with a strong donor diethylamino group **19b** possessed the most-red shifted absorption spectrum (460 nm) (Figure 7). Compound **19b** represents the most extended donor-π-acceptor unit in phenazines discussed thus far, originating from the diethylamino donor to the pyrazine acceptor through an alternate benzene-imine-benzene linkage. This would allow for extensive charge delocalization. σ_p values for the closely related $-NMe_2$ group is -0.83, which is also the highest among all donor groups discussed thus far.[22] The distribution of the charges in the frontier molecular orbitals in **19b** also supports this statement where the HOMO was

distributed over the entire molecule although with higher electron density on the electron rich phenyl rings, the LUMO was only localized in the phenazine moiety.[24] Greater extent of conjugation in the salen bearing the napthyl moiety **19c** rendered its absorption spectra more red-shifted (420 nm) in contrast to molecule **19a** (403 nm). The HOMO-LUMO energy gap for the three molecules also parallel their UV-visible optical spectra (2.92 eV for **19b**, 3.06 eV for **19c** and 3.30 eV for **19a**).[24] Since salens serve as ligands for several important metal ions, these phenazine based ligands could be useful in spectroscopic chemosensing of metal ions in solutions.

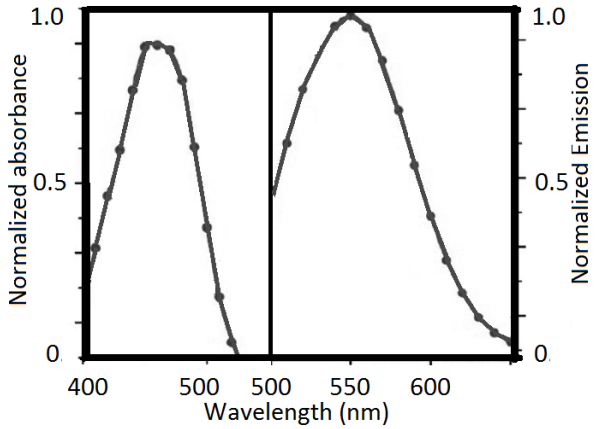

Figure 7. UV-visible spectrum (left) of **19b** and it corresponding fluorescence spectrum (right) in acetonitrile; adapted from reference 24.

2.2 Phenazine-based probes as chemosensors/chemodosimeters for analyte sensing

The synthesis and optical properties of fluorescent phenazines having been discussed, it is important look at their applications as sensors of solution analytes. Bunz *et. al.* have described the synthesis of a triazole bearing phenazine **24** which was used as a fluorescence turn-off chemosensor for Ag^{+} ions.[6] The synthesis (Scheme 5) proceeded through coupling between di-alkynylated *o*-phenylene diamine **20** and *o*-benzoquinone **21** to construct the phenazine core **22**. This was followed by a copper catalyzed 'click reaction' between the phenazine alkyne **22** and alkoxy substituted azide **23** to yield the triazole bearing phenazine **24**. Since creating a system capable of analyte sensing in aqueous solution was important, the long chain triethyleneoxy group was incorporated. The UV-visible spectrum of **24** showed strong absorption in the region of 400-450 nm in dichloromethane and was blue shifted by about 20 nm in water, while the emission spectrum was red-shifted on proceeding from dichloromethane to water (559 to 569 nm) (Figure 8A, 8B). Phenazine **24** exhibited high degree of binding selectivity for Ag^{+} ion as indicated by the extent of phenazine fluorescence quenching (Figure 8C) over Na^{+}, K^{+}, Li^{+}, Mg^{2+}, Ca^{2+}, Zn^{2+}, Cu^{2+}, Ni^{2+}, Hg^{2+}, Cd^{2+}, and Pb^{2+} ions, when a dilute solution of metal ions was added incrementally to a solution of **24** in water. The presence of the triazole unit was also found to be necessary as the peralkynylated starting phenazine **22** was also tested for its

metal binding ability and it exhibited fluorescence quenching only at very large excess concentrations of the analyte.[6]

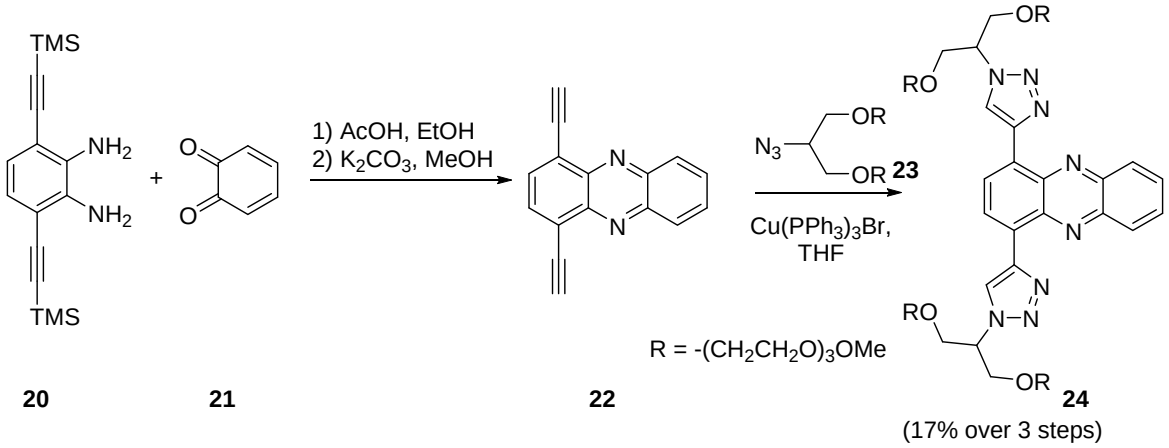

Scheme 5. Synthesis of triazole phenazine containg a silver binding pocket.

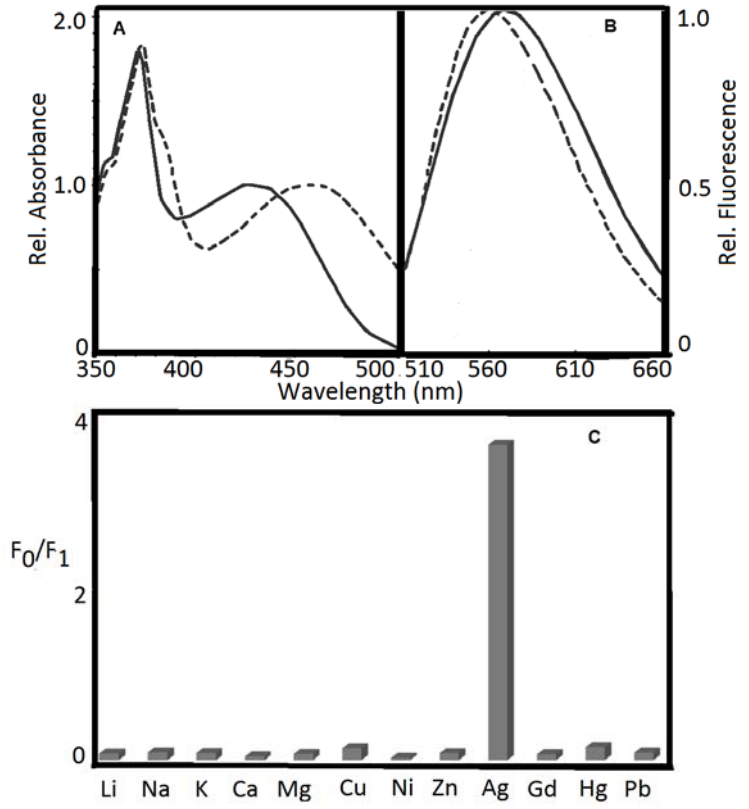

Figure 8. (A) UV-visible spectrum of **24** in DCM (dashed line) and water (solid line); (B) Fluorescence emission spectrum of **24** in DCM (dashed line) and water (solid line); (C) Plot of F_0/F_1 (ratio of initial to final fluorescence intensity after metal ion addition) vs metal ions added showing high degree of fluorescence quenching upon Ag^+ ion addition; adapted from reference 6.

The nature of the binding pocket with Ag^+ ion was investigated using theoretical calculations and also NMR titration methods to elucidate that the Ag^+ ion was ligated both by the pyrazine nitrogen atom and also the triazole nitrogen forming a cyclic six-membered coordination complex. The lowest energy conformation of **24** in absence of any Ag^+ ion is indicated in Scheme 6 by structure **24A**, whereby the nitrogen based lone pair-lone pair repulsion between the pyrazine and triazole nitrogen atoms would be minimized. The rotamer **24B** providing the metal ion binding pocket was 9 kcal mol^{-1} higher in energy on account of the said electron-electron repulsions.

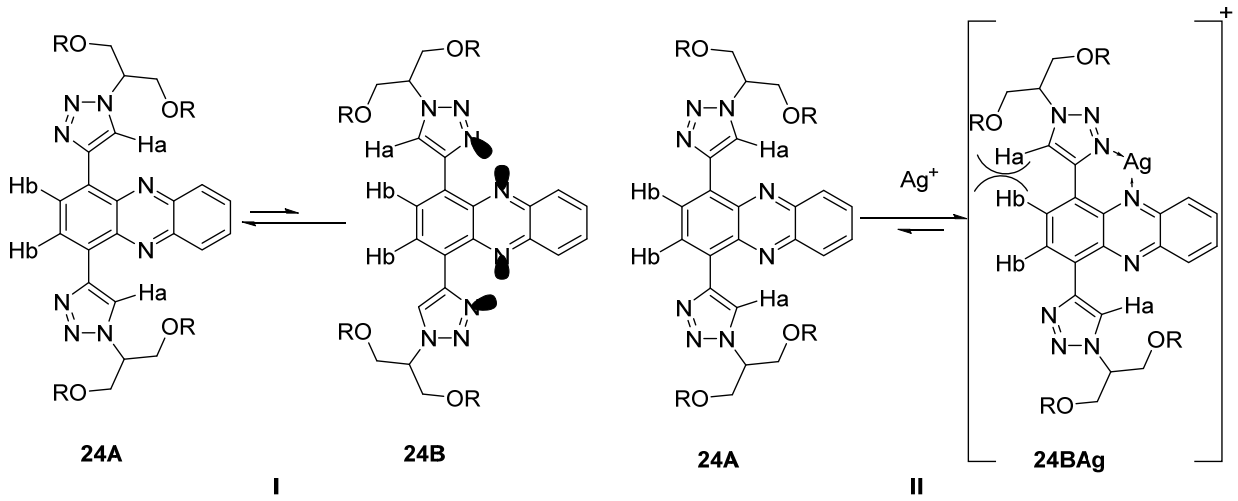

Scheme 6. Rotamers **24A** and **24B** in equilibrium: (I) in absence of Ag+ion, (II) in presence of Ag+ ion.

In 2D-NOESY NMR analysis it was revealed that only upon binding of Ag^+ ion a through space H-H correlation was found between the triazole H-atom (Ha) and the phenazine-2-position H-atom (Hb) as depicted in rotamer structure **24BAg**. This added further credence to the indicated binding mode of the Ag^+ ion to the triazole-phenazine sensor. Given the many industrial applications of silver and its persistence in the environment, development of such a selective and sensitive water soluble chemosensor with an emission signal in the 570 nm range (away from background emission of biological tissue) is indeed valuable.

The optical properties of 2,3-diaminophenazine **4** having been described before, utilization of the same for colorimetric and fluorimetric detection of Cu^{2+} ion at the sub-nano molar level has also been achieved by Udhayakumari *et. al*.[25] When a dilute acetonitrile solution of **4** was added to differently colored aq. solutions of metal ions (Fe^{3+}, Co^{2+}, Ni^{2+}, Cu^{2+}, Zn^{2+}, Cd^{2+}, Pb^{2+}, Hg^{2+}, Mn^{2+}, Sn^{2+}, Cr^{3+}), only in case of the Cu^{2+} solution a decolorization was observed (green to colorless), indicating its highly degree of selectivity for Cu^{2+} ion.[21] Additionally to the Cu^{2+} ion solution containing **4** were added the other mentioned cations, but no color changes were observed. This indicated that the complex formation between **4** and Cu^{2+} ion was very stable.

The UV-vis absorption spectrum of **4** bearing a broad peak centered on 419 nm disappears completely upon addition of an aq. solution of Cu^{2+} ion (Figure 9A). Only in the region below 250 nm there is marginal increase in absorbance. This was explained on the basis of theoretical calculations using DFT optimized structures of the free ligand and its metal complex to elucidate its HOMO and LUMO levels. It was found that the HOMO-LUMO gap in case of **4** was 2.96 eV while after complex formation with Cu^{2+} ion it increased to 4.149 eV. This was due to stabilization of the HOMO as a result of complex formation with the metal center and further LUMO destabilization. Similarly, the fluorescence emission band of **4** at 500 nm also disappeared upon addition of a dilute solution of Cu^{2+} ion and this fluorescence quenching was once again selective only for copper and independent of the counter anion (Figure 9B).

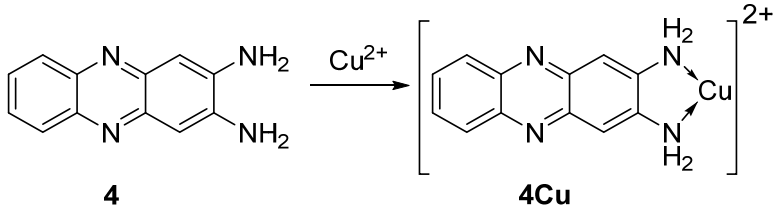

Scheme 7. Chemosensing of Cu(II) ion by **4**.

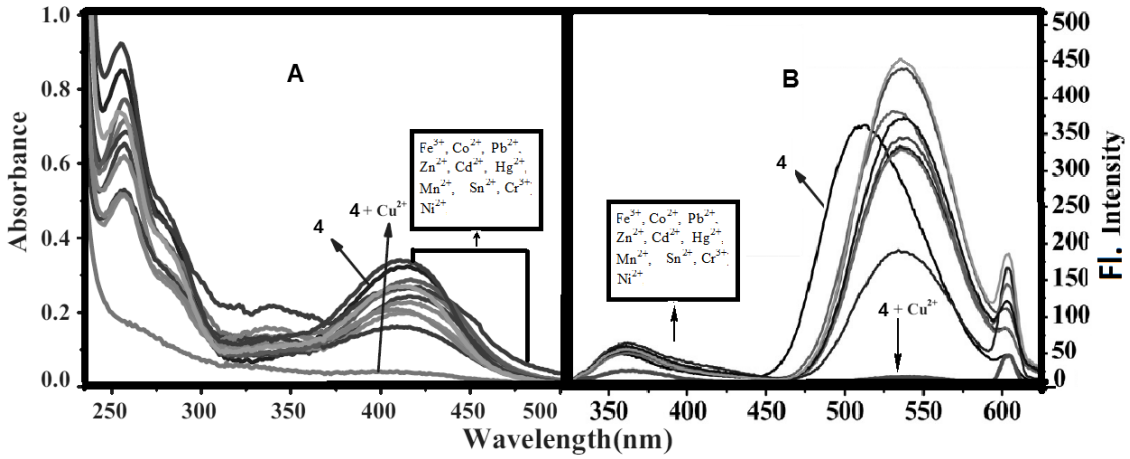

Figure 9. (A) UV-visible spectrum of **4** and hypsochromically shifted UV-visible spectrum of **4Cu(II)** complex in acetonitrile indicating selective recognition of Cu(II) by **4**; (B) Fluorescence emission spectrum of **4** and quenching of fluorescence upon formation of **4Cu(II)** complex in acetonitrile; adapted from reference 25.

Job's plot studies indicated formation of a 1:1 complex with copper (II) ion utilizing the 2,3-diamino groups as the donor atoms and the detection limit was measured to be 0.23 sub-nM. This fluorescence quenching was only observed within a pH range of 4-8 indicating that outside this pH range the phenazine-copper complex was not formed. The paramagnetic nature of Cu^{2+}

ion was attributed to be the reason for the fluorescence quenching observation, whereby the forbidden intersystem crossing (ISC) between the excited singlet state and low lying triplet state of the phenazine would be allowed, leading to a non-radiative relaxation.[25]

Complementary to the work done on using phenazines for cation detection, they have also been researched for chemosensing of anions in solution. Chauhan *et. al*. reported synthesis of a colorimetric receptor possessing bis-urea appended phenazine and its application in sensing and differentiation between fluoride, acetate and dihydrogen phosphate anions.[7] The molecule was synthesized (Scheme 8) by refluxing a DMF/THF solution of 2,3-diamino phenazine with phenyl isocyanate. While the urea motif served as the anion receptor, the phenazine portion was the chromogenic signaling subunit exhibiting the optical spectral changes sensitive to the analyte anion. Upon addition of a number of anion aq. solutions (chloride, bromide, iodide, hydrogen sulfate, dihydrogen phosphate, acetate) the color of the DMSO solution of compound **25** changed to red only for fluoride and to different shades of orange for dihydrogen phosphate and acetate. All changes occurred at the micromolar to millimolar levels of anion concentration. The UV-vis spectrum of **25** red-shifts from the 400 nm peak to a new broad signal at 510 nm with incremental amounts of fluoride anion addition, while in case of the fluorescence emission spectrum, the signal at 610 nm for **25** is red-shifted to 645 nm bearing an isobestic point at 625 nm with intensity enhancement upon addition of fluoride ion (Figure 10). The fluoride on account of its small size and high electronegativity is able to interact most with the urea moiety through H-bonding, which in turn modulates the extent of charge transfer occurring in **25** resulting in the observed optical spectral changes.[7]

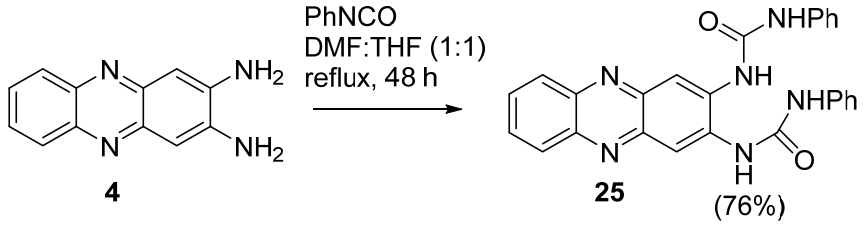

Scheme 8. Synthesis of 1-Phenyl-3-[3-(3-phenyl-ureido)-phenazin-2-yl]-urea based anion sensor.

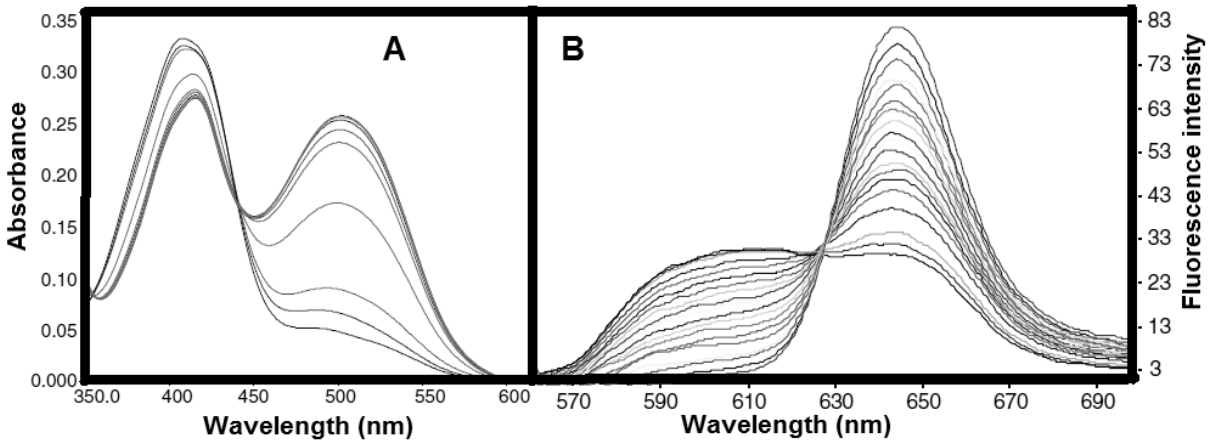

Figure 10. (A) UV-visible spectral changes of **25** upon incremental addition of fluoride anion in DMSO; (B) Fluorescence emission spectral changes of **25** upon incremental addition of fluoride anion in DMSO; adapted from reference 7.

The utilization of the chromogenic properties of 2,3-diaminophenazine **4** was extended by Wang *et. al.* by preparation of a fluorimetric imidazole extended 2,3-diaminophenazine sensor **27**, also bearing an electron deficient perfluorophenyl group.[26] The compound was prepared as shown in Scheme 9 by fusing a solid mixture of **4**, the perfluorophthalic anhydride **26** and zinc acetate. The compound was fully characterized by NMR, MS, IR and single crystal X-ray diffractometry, which showed a fully planar structure, indicating presence of an H-bonding interaction between the imidazolo hydrogen atom and the perfluorophenyl ring. Upon addition of dilute solutions of different anions (F^-, Cl^-, Br^-, I^-, NO_3^-, HSO_4^-, ClO_4^-, BF_4^-) to the acetonitrile solution of **27**, only in case of fluoride a colorimetric, UV-spectrophotometric and fluorimetric response was observed. The UV-visible spectrum of **27** possessed its highest absorption band at 465 nm, which was replaced upon addition of fluoride by a weak broad band centered on 540 nm and the color of the solution of **27** in acetonitrile changed from yellow to orange. In the fluorescence spectra of **27** the main emission signal at 512 nm was diminished in intensity to almost half value and a new weaker band appeared at 637 nm.

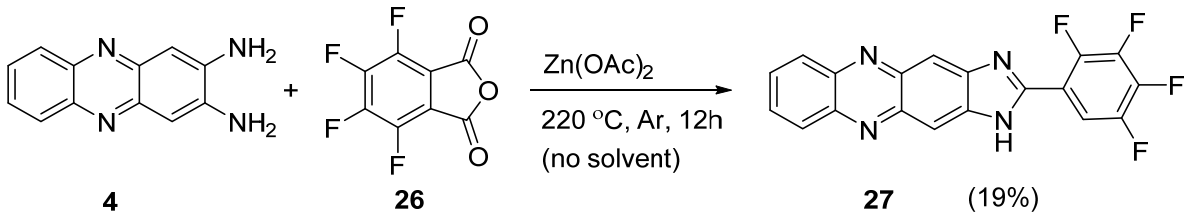

Scheme 9. Synthesis of imidazole-extended phenazine based anion sensor.

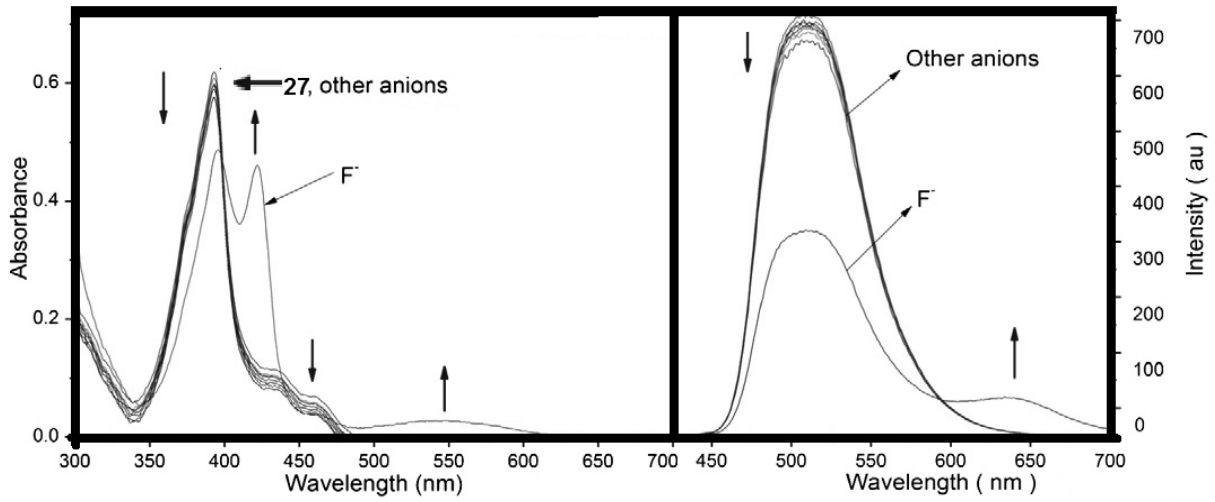

Figure 11. (Left) UV-visible spectral changes of **27** upon addition of fluoride and other anions anion in acetonitrile, (Right) Fluorescence emission spectral changes of **27** in acetonitrile upon addition of fluoride and other anions; adapted from reference 26.

Job's plot analysis revealed formation of a 1:1 complex between the fluoride anion and compound **27**. The nature of interaction between fluoride and **27** was investigated by proton NMR spectroscopy and it was found that upon addition of the fluoride, the signal for the imidazolo NH disappears which suggests that it could be involved with H-bonding with the F^- anion. Also signals for the phenazine moiety H-atoms shift upfield due to increased electron density transfer from the imidazole ring to the phenazine itself. This greater extent of charge delocalization could possibly explain the appearance of the red-shifted absorbance peak in the UV-vis spectrum of **27**. The important feature of this work was that the selectivity of **27** towards F^- ion remained unchanged even when it was treated with an equimolar mixture of F^-, Cl^-, Br^-, I^-, NO_3^-, HSO_4^-, ClO_4^-, BF_4^- anions.[26]

Certain imidazole-phenazines have also been used as a chemosensor for Fe^{3+} ion in DMSO solution. The detection lower limit was found to be at 4.8×10^{-6} M concentration of Fe^{3+} in DMSO and it showed selectivity for Fe^{3+} in presence of other cations including Hg^{2+},Ag^+, Ca^{2+}, Cu^{2+}, Co^{2+}, Ni^{2+}, Cd^{2+}, Pb^{2+}, Zn^{2+}, Cr^{3+}, and Mg^{2+}.[27] The detection was possible due to a fluorescence turn-off behavior of the probe, whereby complexation with Fe^{3+} diminished its fluorescence quantum yield Φ from 0.48 to 0.03 at the emission maximum of 533 nm. Filter paper strips coated with the sensor molecule as a test kit also exhibited a colorimetric turn-off response when drops of Fe^{3+} solution in DMSO were added to it, providing a means of practical detection of Fe^{3+} ions.

A furanyl-2-subtituted imidazole-phenazine was also reported as reversible sulfur free selective sensors of Hg^{2+} ions in presence of Fe^{3+}, Ca^{2+}, Cu^{2+}, Co^{2+}, Ni^{2+}, Cd^{2+}, Pb^{2+}, Zn^{2+}, Cr^{3+}, and Mg^{2+} ions, with a detection lower limit of 1.6×10^{-7} M of Hg^{2+} ions.[28] Once again a fluorescence turn-off behavior in presence of the analyte was attributed to the sensory response.

The lack of a coordinating sulfur atom in the molecule proved to be an advantage in terms of its reversibility, since the Hg^{2+} ion sensed by the probe through coordination with the pyrrole and imidazole rings could be removed as HgS, rendering the probe available for further use. Filter paper strips coated with the sensor molecule as a test kit also exhibited a colorimetric turn-off response when drops of Hg^{2+} solution in DMSO were added to it, providing a means of its practical detection.

Several examples of phenazine based chemosensors having been discussed,[6,7,25-28] it is also noteworthy that phenazine based NIR active chemodosimeters for cyanide ion has also been prepared and tested successfully.[29] The synthesis of compound **31** is outlined in Scheme 10 whereby the phenazine core **28** is reduced and alkylated to convert it into an electron donor center in **29**. Vilmeieyer Haack formylation generates the diformyl intermediate **30** and final Knoevenagel condensation with malononitrile produces the acceptor-donor-acceptor type probe molecule **31**.

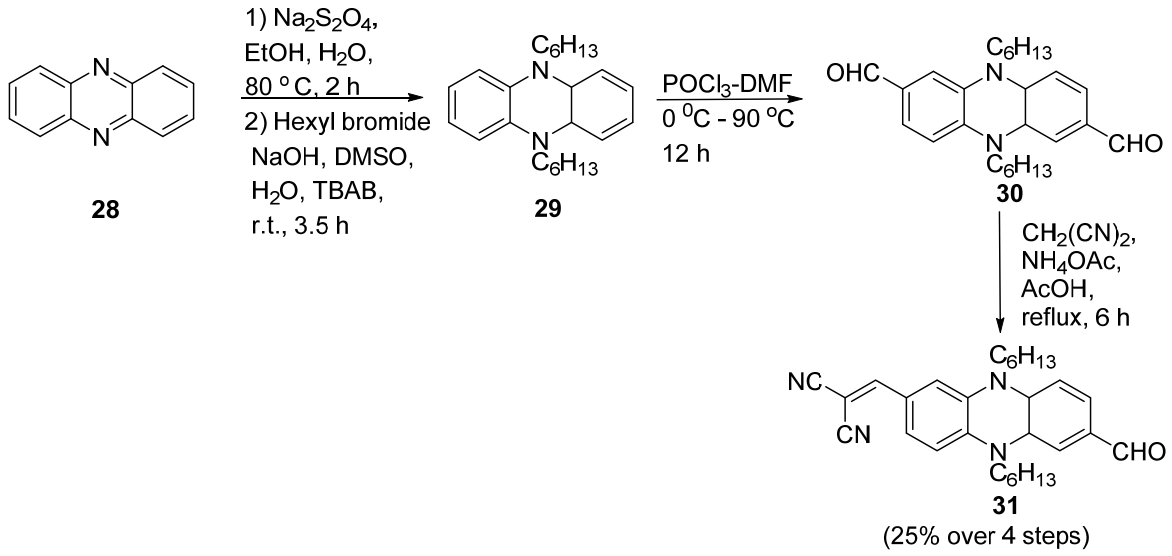

Scheme 10. Synthesis of phenazine based cyanide chemodosimeter.

The UV-visible spectrum of **31** has peaks at 570, 452, 360, and 293 nm of nearly equal intensity (Figure 12A). With incremental amounts of cyanide anion addition to an acetonitrile solution of **31**, the 293 nm peak is enhanced, while the 570 nm peak disappears. Existence of an isobestic point at 316 nm indicated the presence of a new species due to cyanide addition. The saturation is reached at 3.2 equivalents of cyanide concentration. A plot of ratio of absorbances at 293 nm and 452 nm with increasing cyanide concentration gave a sigmoidal curve (Figure 12A inset). The fluorescence emission spectrum of **31** exhibited a NIR peak at 710 nm and upon addition of upto 3.2 equivalents of cyanide anion this peak was ratiometrically blue-shifted to 630 nm with an isoemissive point at 664 nm (Figure 12B). This suggested development of a new

fluorophore due to cyanide addition to **31**. The limit of detection was 0.2 nM which was lower than the 0.2 ppm limit for cyanide set by United States Environment Protection agency.

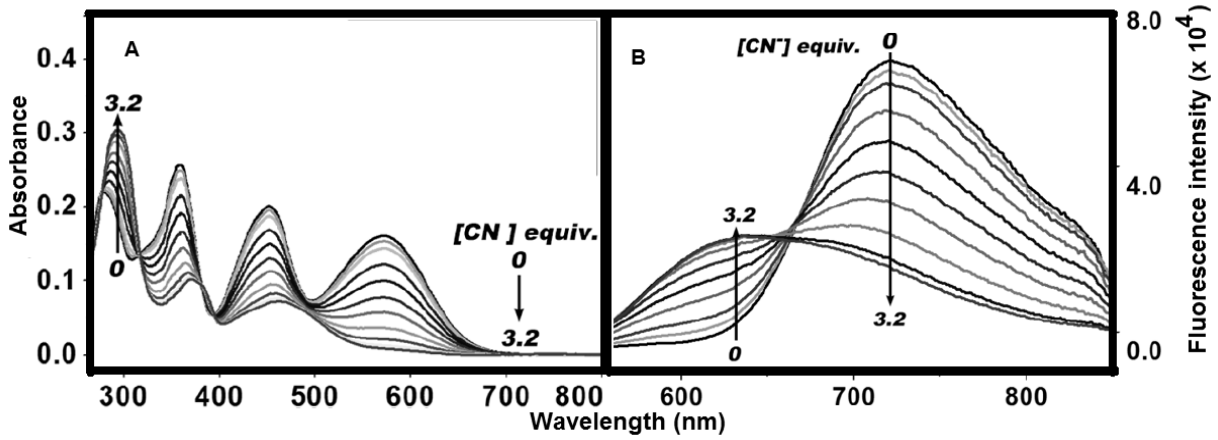

Figure 12. (A) UV-visible spectral changes of **31** in acetonitrile upon incremental addition of cyanide anion; (B) Fluorescence spectral changes of an acetonitrile solution of **31** upon incremental addition of up to 3.2 equiv cyanide anion; adapted from reference 29.

A proton NMR spectrum of **31** was recorded in CD_2Cl_2 and upon addition of cyanide anion, the signal at 7.96 ppm for the vinylic proton is upfield shifted to 4.28 ppm. This indicates that the dicyanovinyl moiety is acting as a Michael acceptor group for nucleophilic attack of the cyanide anion to form the new species as indicated in Figure 13.

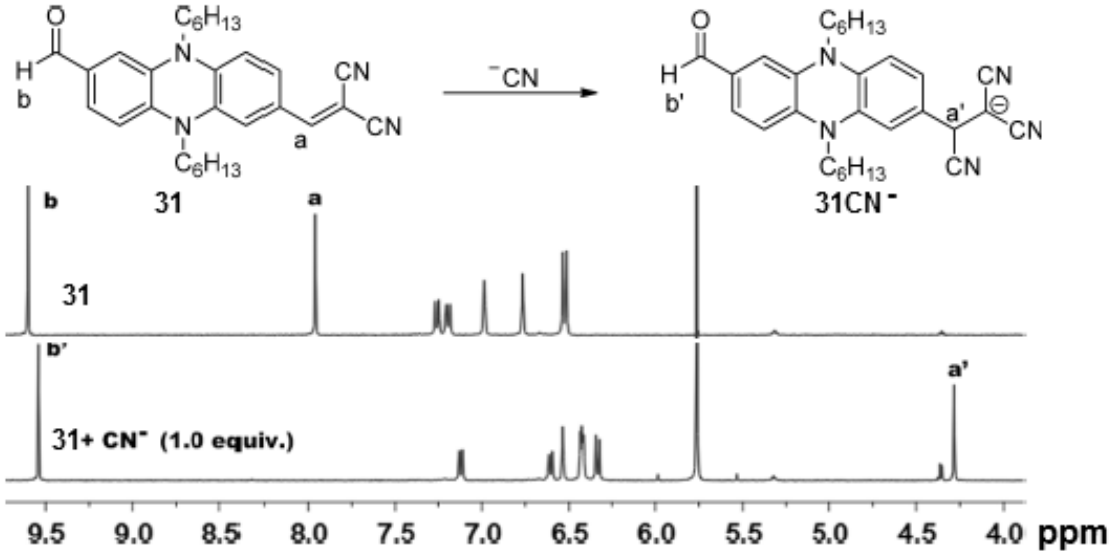

Figure 13. ^{1}H NMR spectrum of **31** in CD_2Cl_2 (top) and after addition of 1.0 equiv. of cyanide anion (bottom); adapted from reference 29.

The blue shifting in the optical spectra upon chemodosimetric cyanide detection was also explained through theoretical analysis of the frontier molecular orbitals of compound **31**. In case of **31** there were two ICT mechanisms in operation from the central electron-rich nitrogen atoms to the peripheral dicyanovinyl and formyl groups. The LUMO for **31** was found to be mostly localized on the dicyanovinyl group, but upon cyanide addition the LUMO of the adduct was now localized onto the formyl group only, which was also of higher energy than the LUMO of **31**. Hence only one ICT mechanism is now operational from the central nitrogen to the formyl group, thereby effecting a blue shifting of the absorption spectrum. The selectivity of compound **31** for CN^- ion in presence of possible interfering ions such as F^-, Cl^-, Br^-, I^-, PO_4^{3-}, CO_3^{2-}, SO_4^{2-}, NO_3^-, SCN^-, AcO^-, HSO_3^-, NO_2^-, and HCO_3^- was also tested by mixing in 10-fold excess in presence of a solution of **31** and CN^- ion and the results obtained were very satisfactory, since there was no change in the ratiometric optical response and colorimetric response of **31** towards cyanide anion. Additionally, even though **31** was insoluble in water, a solution of **31** in small amount of acetonitrile could be added to an aq. solution of cyanide ion for the chemodosimetric measurements.[29]

2.3 Phenazines in organic photovoltaics

Red-absorbing and emitting phenazine based polymers have also been investigated in organic photovoltaics for artificial light harvesting applications.[12] This is important since greater than 50% of the solar radiation incident on earth falls in the visible to NIR region.[30] Suitable materials with low bandgap implying red-shifted absorptions can be created by incorporation of donor and acceptor groups in the molecule, whereby the HOMO is delocalized over the entire molecule though extensive charge transfer, but the LUMO is mostly centered on the acceptor moiety. Phenazines and thiadiazole extended phenazines with two thiophene units were synthesized as shown in Scheme 11 as donor-acceptor-donor charge transport materials.[31]

The thiophene units functioned as electron donor segments while the phenazine units behaved as the electron accepting segments. It was revealed through theoretical calculations and cyclic voltametric measurements that the dihedral angle between the phenazine and thiophene rings played an important role in the extent of orbital delocalization and consequently bandgap reduction in the materials. Compound **37** bearing the thiadiazole moiety was almost perfectly planar with nearly zero dihedral angle due to stabilizing interaction between the thiophene-3H and the thiadiazole nitrogen and the attractive interaction between the thiophene-S and pyrazine-N. In contrast the dihedral angle for compound **34** was nearly 15 degrees. The HOMO-LUMO gap for **37** was 1.43 eV while for compound **34** was 2.19 eV, a fact that could be attributed to the higher degree of orbital overlap in **37** due to its planarity as compared to **34**. The UV-visible absorption spectrum of **34** (Figure 14) exhibited its longest wavelength peak at 485 nm with an extinction coefficient of 14000 $cm^{-1}M^{-1}$ while the thiadiazole extended phenazine derivative **37** possessed the longest wavelength absorption peak in the NIR region at 745 nm.

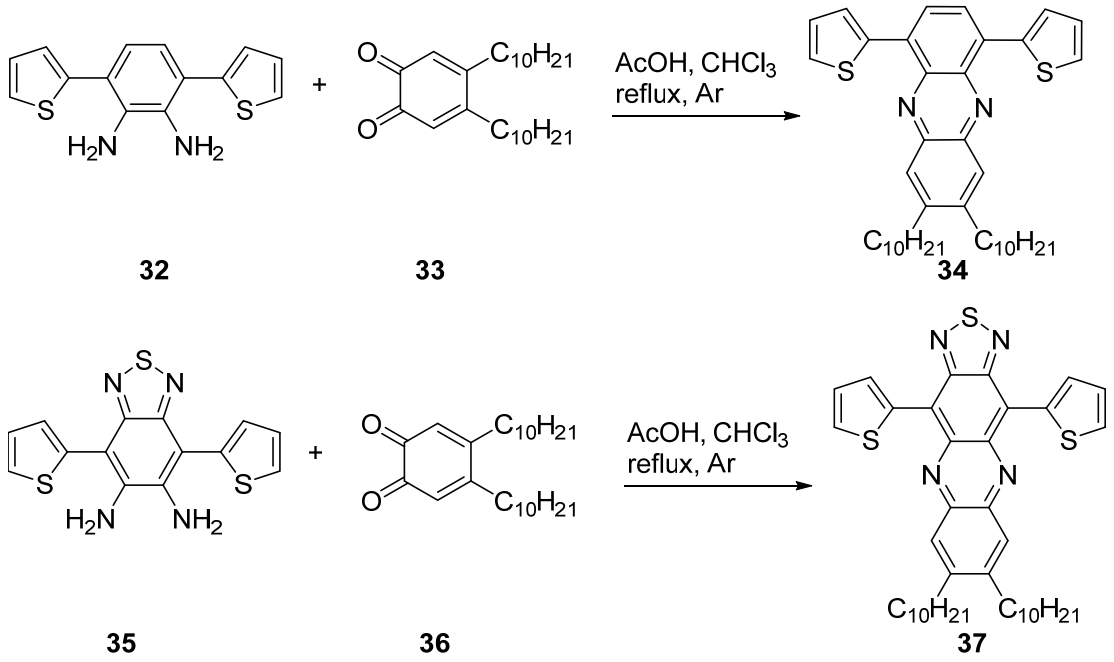

32 **33** **34**

35 **36** **37**

Scheme 11. Synthesis of thiophene appended phenazines.

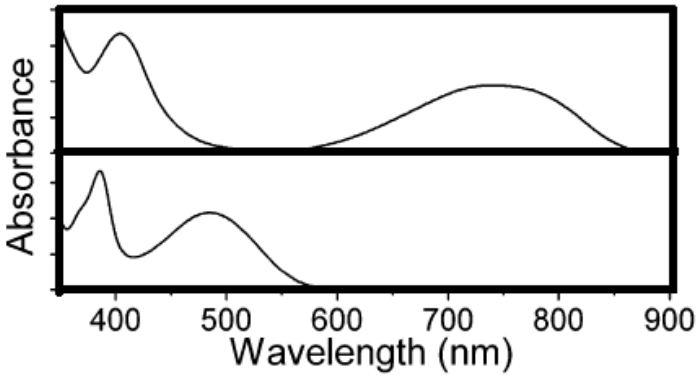

Figure 14. UV-visible spectra of **37** (top) and **34** (bottom) in $CHCl_3$; adapted from reference 31.

On account of its low bandgap the thiadiazole compound **37** was used in a bulk heterojunction (BHJ) solar cell as an interfacial nanolayer between the poly(3-hexylthiophene (P3HT) and [6,6]-phenyl-C61-butyric acid methyl ester (PC60BM) photoactive layer (1:1 weight ratio) and Al cathode. The thickness of the contact nanolayer of thiadiazole phenazine **37** deposited on the photoactive layer by spin-coating an acetonitrile solution of **37** was found vary between 2.4-6.0 nm. The highest power conversion efficiency (PCE) of the devices with the n-type interfacial nanolayer (6.0 nm) was 1.36% while the control device without the interfacial nanolayer possessed a PCE of 1.19%. Hence by including the low bandgap electron deficient small molecule **37** bearing a phenazine acceptor core, PCE of the device was increased by about 13%. The BHJ solar cell bearing the thiazdiazole phenazine contact layer exhibited a lower

series resistance (R_s) and higher shunt resistance (R_{sh}) than the control cell indicating better electron extraction and transport through the contact layer.[31]

The carbazole group is generally considered to be a good electron donor group in organic photovoltaics. However, when attached to a highly electron-withdrawing benzophenazine unit on the nitrogen in the carbazole group it behaves as a good electron acceptor.[12] Such modifications could also reduce the bandgap in materials to be evaluated for photovoltaic applications. The synthesis of carbazole-linked benzophenazine and its polymerization with a well-known electron donor group benzo[1,2-*b*:4,5-*b*']dithiophene (BDT) for photovoltaic applications was reported.[12] Scheme 12 shows the preparation of the modified carbazole phenazine acceptor **42** and its polymerization through double Stille coupling with the distannyl BDT donor group **43** to give rise to the carbazole-phenazine containing polymer **44**. For the purpose of comparison distannyl BDT **43** was also polymerized with N-alkyl carbazole **45**, to study the effect of phenazine incorporation.

The UV-vis spectra of a thin film of polymer **44** and corresponding polymer of N-alkyl carbazole **46** are shown in Figure 15. While for the non phenazine polymer there is only one strong absorption peak at 430 nm, the phenazine containing polymer showed two clear absorption bands at 428 nm and 660 nm. The 430 nm peak corresponded to the π-π* transition of the polymer chain and the 660 nm peak arises from an intramolecular charge transfer (ICT) from the electron donor BDT unit to the electron accepting phenazine carbazole moiety.[12] The measured bandgap from theoretical calculations for the phenazine polymer **44** was 1.56 eV, while for the non-phenazine polymer **46** a much higher value of 2.41 eV was found, which was unsuitable for any photovoltaic applications. Hence the presence of the phenazine does play a role in reduction of band gap and rendering the polymer more useful for light harvesting purposes. Presence of the electron withdrawing phenazine group in **44** also rendered it oxidatively more stable as compared to the non-phenazine carbazole polymer. This was revealed from the oxidation potential value of **44** (-5.48 eV) measured by cyclic voltametric measurements, which was more negative than the corresponding value for the non-phenazine polymer **46** (-5.21 eV). This was due to the more negative HOMO energy level of **44** arising due to the presence of the electron withdrawing phenazine moiety than that of the non-phenazine polymer.

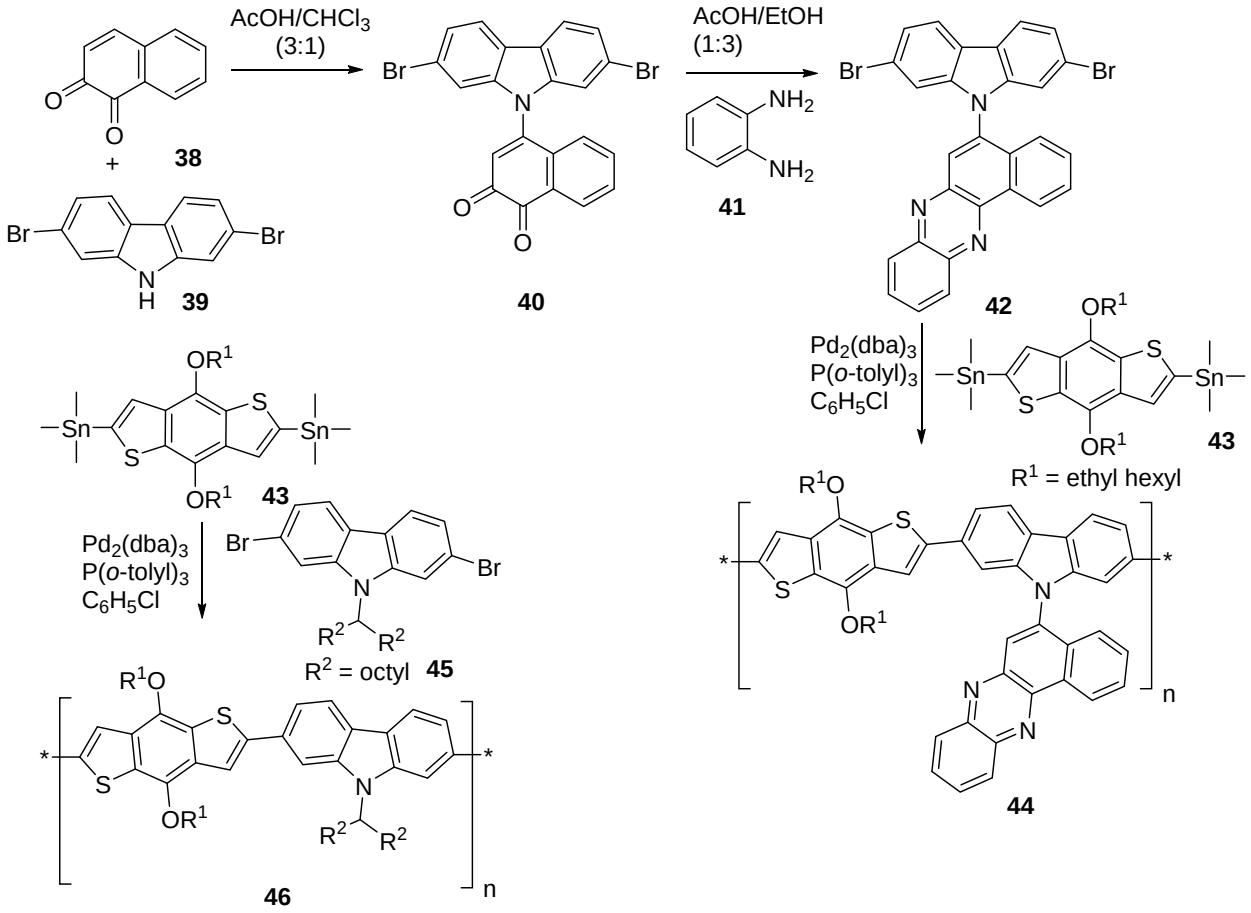

Scheme 12. Synthesis of benzophenazine-carbazole- benzodithiophene containing polymer.

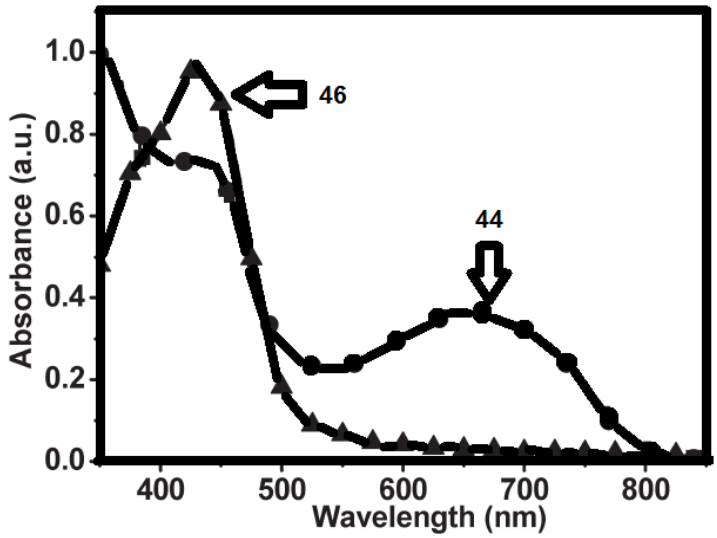

Figure 15. UV-visible spectra of polymer films of **44** and **46** on a quartz plate; adapted from reference 12.

The thin-film transistor (TFT) characteristics of the prepared polymer films were evaluated to determine whether they would behave as a *p*-type or *n*-type transistor, by fabricating the films over a silicon wafer. Both the phenazine containing polymer **44** and alkyl carbazole based polymer **46** showed *p*-type transistor characteristics with hole mobilities of 2.0×10^{-4} and 3.6×10^{-4} cm^2 $V^{-1}s^{-1}$ respectively. On account of lower bandgap in phenazine containing polymer **44** the hole transport mobility value is higher than the non-phenazine polymer. Photovoltaic devices based on the prepared polymer films were fabricated using them as *p*-type electron donors, and [6,6]-phenyl C71-butyric acid methyl ester ($PC_{71}BM$) as an *n*-type acceptor. The optimum device performance (2.33% PCE) was obtained for the phenazine containing polymer **44** and $PC_{71}BM$ in a 1:2 ratio with PEDOT:PSS as the hole transport layer (HTL) and a MoO_3 layer to buffer the acidity of the PEDOT:PSS layer. In contrast the best performance of the non-phenazine polymer was PCE of only 0.25%.[12]

In addition to being present as electron withdrawing subunits in polymeric materials prepared for photovoltaic applications, phenazine based small molecules have also been prepared with electron donor and acceptor groups, which have found use in dye sensitized solar cells (DSSCs). A near-infrared (NIR) organic sensitizer 53 (Scheme 13) with a dithieno-phenazine moiety containing a triaryl amine electron donor and a cyano acrylic acid based electron withdrawing unit was synthesized for quasi-solid-state dye-sensitized solar cells (DSSCs).[11] The synthetic scheme is outlined in Scheme 13.

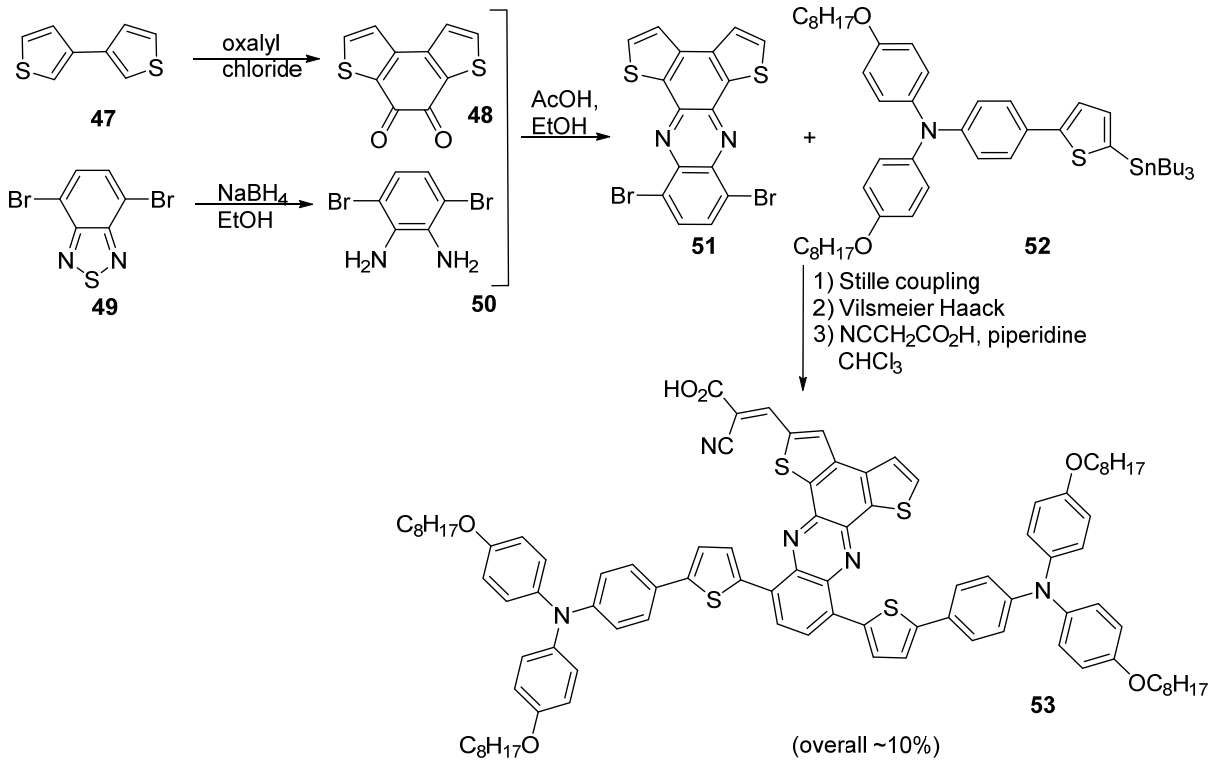

Scheme 13. Synthesis of phenazine bridged donor-acceptor sensitizer.

The UV-visible absorption spectrum of compound **53** is outlined in Figure 16. In addition to the band above 400 nm arising from π-π* transitions of the conjugated molecular backbone, another prominent broad absorption band was found centered at 629 nm. This corresponded to the intramolecular charge transfer (ICT) transition between the donor triaryl amino group and the acceptor cyano acrylic acid unit attached through the phenazine moiety.[11] The high degree of co-planarity of the dithieno-phenazine allows for effective orbital overlap and charge transfer between the donor and acceptor portions of the molecule. Hence a moderately intense absorption band in the red region (629 nm) could be found in **53**, a fact that is significant for light harvesting applications. When adsorbed onto a mesoporous TiO_2 film the UV-visible spectrum is blue shifted to 621 nm due to deprotonation of the anchoring -CO_2H group resulting in reduced electron withdrawing capability. The bandgap as measured from cyclic voltametric measurements was found to be 1.60 eV, which was in the acceptable range for photovoltaic applications.

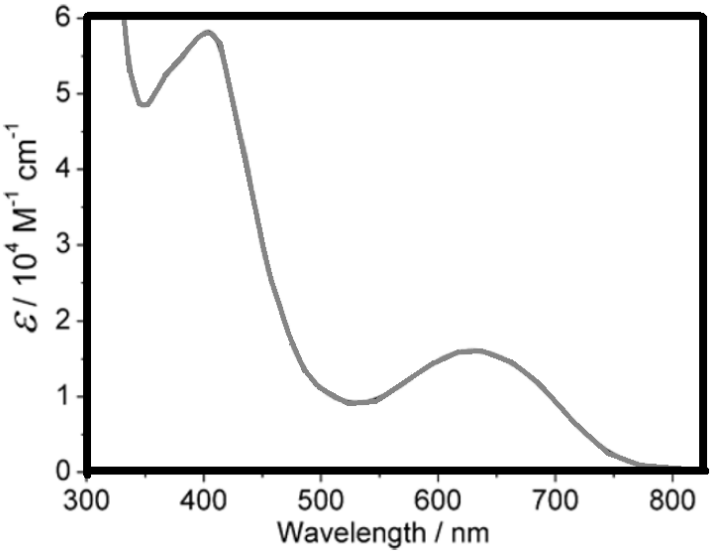

Figure 16. UV-visible spectrum of **53** in toluene; adapted from reference 11.

The performance of compound **53** as a photo-responsive dye in a TiO_2 solar cell was evaluated by preparing cocktail-type quasi-solid-state DSSCs co-sensitized with compound **53** and another known dye with a strong absorbance band at 542 nm[11] in a 2:8 molar ratio. The co-sensitization was done so that the dye cocktail would have capability to absorb sunlight in the entire visible to NIR region. This DSSC with the dye mixture obtained an acceptable PCE value of 8.04% and the incident photon to current conversion efficiency (IPCE) was as high as 85%.[11] The significance of these results lie in the fact that even the best recorded PCE value of 12.3% was obtained by using a heavily modified Zn-porphyrin,[32] i.e. a metal complex, which often are expensive to produce and may have complex synthetic protocols. Thus the compound **53** a

metal-free all organic sensitizer being successfully used in a DSSC, opens up possibilities of cost-effective and environmentally friendly materials becoming available for DSSC applications.

An important feature of DSSC sensitizers is that their structure should be such so as to prevent π–π stacking between the sensitizer molecules and prevention of the I_3^- ions of the electrolyte from reaching the TiO_2 surface. 11,12-Bis(hexyloxy) dibenzo[*a,c*]phenazine based molecule was proposed to be a photosensitizer which could have broad panchromatic UV-visible absorption due to its extensive conjugation. Additionally the hexyloxy groups located orthogonally to the molecular framework could prevent sensitizer stacking and act as a blocking group for I_3^- ions of the electrolyte from reaching the TiO_2 surface.[33] The synthesis of sensitizer **61** based on a dibenzophenazine moiety is described in Scheme 14.

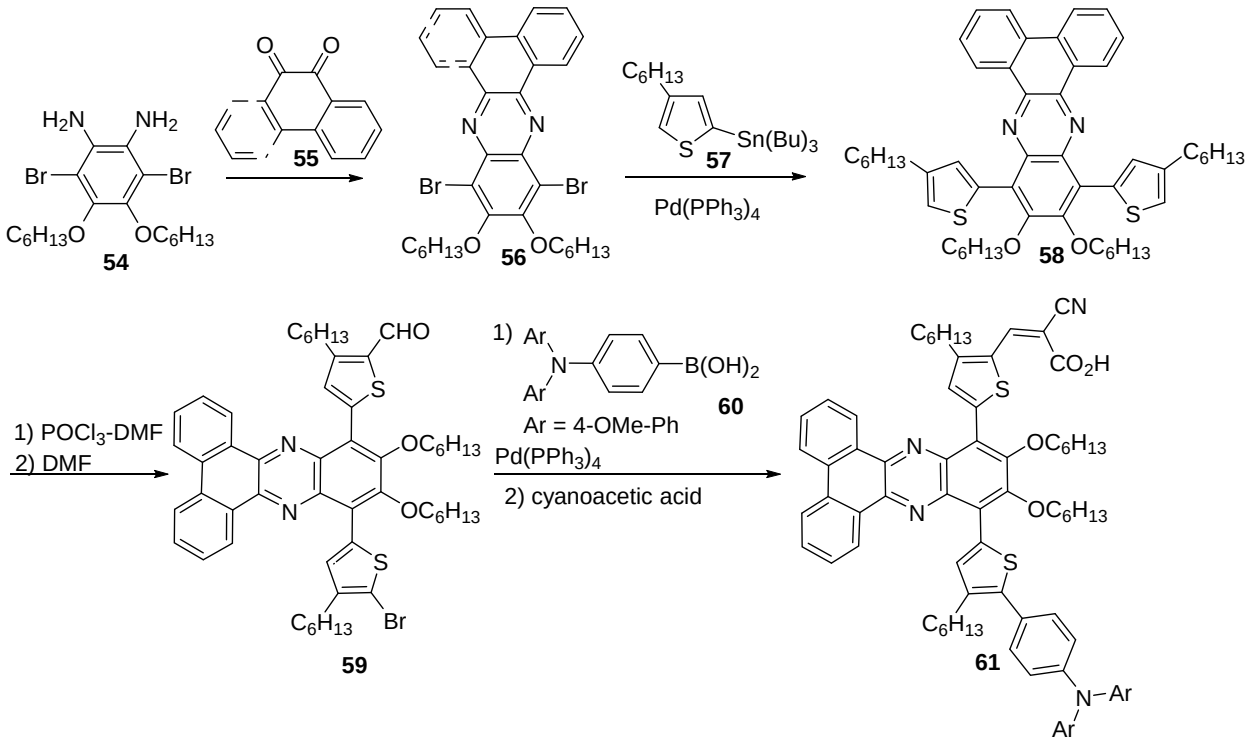

Scheme 14. Synthesis of dibenzophenazine linked donor-acceptor sensitizer.

The UV-visible spectrum spectra of compound **61** exhibits a broad absorption profile with a strong absorption band at 420 nm and a moderate band at 516 nm. While the 420 nm band arises from the π–π* transition of the conjugated molecular backbone, the 516 nm band is attributed to an ICT transition from the triaryl amine donor group to the acceptor cyano acrylic acid group through the phenazine and hexyl thiophene moieties. Upon adsorption onto TiO_2 films the longest wavelength band is red-shifted to 525 nm. This proves that the presence of the bulky benzophenazine moiety prevents intermolecular aggregations leading to energy loss by unwanted molecular interactions.[33] Compound **61** when immobilized onto a TiO_2 surface and evaluated as a photosensitizer thin film for DSSC applications provide PCE value of 7.18%, a respectable

value for non-metallic all organic photosensitizers. The ICPE spectrum showed a broad band response profile and a maximum value of 65% at 525 nm arising from the better light harvesting ability of **61**, due to presence of electron-withdrawing properties of the benzophenazine moiety as well as the strong electron–donating abilities of the methoxyl-substituted triphenylamine unit.

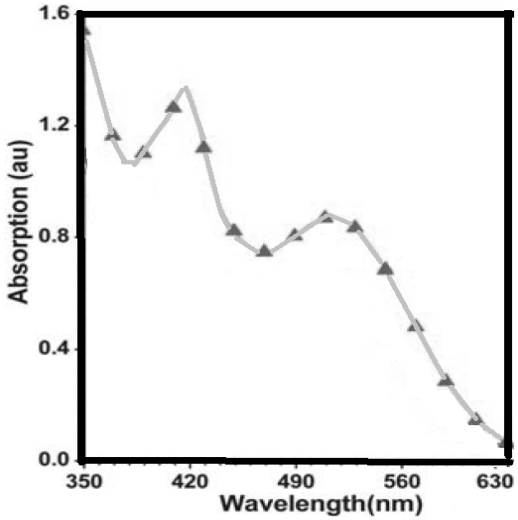

Figure 17. UV-visible spectrum of compound **61** in CH_2Cl_2; adapted from reference 33.

3. Conclusions

The phenazines represent a distinct class of polynuclear heteroaromatic molecules which can be altered chemically to exhibit broad panchromatic absorption and emission spectra. On account of such optical properties they can be used as chemosensors and chemodosimeters for various cations and anions. Complexation with metal ions such as Ag(I) in a specific binding pocket leads to a fluorescence turn-off response which can be used to detect presence of trace Ag(I) in environmental samples. Suitably modified phenazines have also exhibited chemodosimetric behavior towards cyanide anion detection in trace quantities, as reflected in the ratiometric hypsochromic shifting of the original NIR emission spectra of the parent molecule. A thorough theoretical study of a number of modified phenazines indicates presence of an intramolecular charge transfer from peripheral electron donor groups to the central electron deficient pyrazine ring. On account of this behavior it is possible to construct phenazine based donor-acceptor molecules and sensitizers. The utility of phenazine based donor-acceptor molecules was also reflected in their applications as broad spectral dyes in DSSCs and organic photovoltaics mainly due to their ability to produce sensitizers with narrow band gaps and acceptable PCE values up to 8.02%.

On account of their special optical properties there exists scope for further research into designing small molecules bearing donor and acceptor functional groups directly attached to the

phenazine nucleus that could possess NIR optical spectra, which would be sensitive to presence of solution analytes such as cations/anions as well as pollutants such as polycyclic aromatic hydrocarbons and nitroaromatics. Additionally, preparation of more examples of phenazine based low-bandgap containing molecules will also enhance its use in the field of organic photovoltaics.

References

1. Rosenberg, L. *J. Bone Joint Surg. Am.* **1971**, *53*, 69.
2. Winckler, J. *Prog. Histochem. Cytochem.* **1973**, *6*, 1.
3. Yack, J. E. *J. Neurosci.* **1993**, *49*, 17.
4. Huang, Z. Y.; Huang, H. P.; Cai, R. X.; Zeng, Y. E. *Annu. Rev. Biochem. Chim. Acta* **1998**, *374*, 89. http://dx.doi.org/10.1006/abio.1998.2633
5. Terenzi, A.; Tomasello, L.; Spinello, A.; Bruno, G.; Giordano, C.; Barone, G.; *J. Inorg. Biochem.* **2012**, *117*, 103. http://dx.doi.org/10.1016/j.jinorgbio.2012.08.011
6. Bryant, J. J.; Zhang, Y.; Lindner, B. D.; Davey, E. D.; Appleton, A. L.; Qian, X.; Bunz, U. H. F. *J. Org. Chem*. **2012**, *77*, 7479. http://dx.doi.org/10.1021/jo3012978
7. Chauhan, S. M. S.; Bisht, T.; Garg, B. *Tetrahedron Lett.* **2008**, *49*, 6646. http://dx.doi.org/10.1016/j.tetlet.2008.09.033
8. Wang, K.; Jiang, P.; Zhang, Z-G.; Fu, Q.; Li, Y. *Macromol. Chem. Phys.* **2013**, *214*, 1772. http://dx.doi.org/10.1002/macp.201300299
9. Wang, P.; Xie, Z.; Tong, S.; Wong, O.; Lee, C.; Wong, N.; Hung, L.; Lee, S. *Chem. Mater.* **2003**, *15,* 1913. http://dx.doi.org/10.1021/cm0209214
10. Lindner, B. D.; Paulus, F.; Appleton, A. L.; Schaffroth, M.; Engelhart, J. U.; Schelkle, K. M.; Tverskoy, O.; Rominger, F.; Hamburger, M.; Bunz, U. H. F. *J. Mater. Chem. C* **2014**, *2*, 9609. http://dx.doi.org/10.1039/C4TC01992J
11. Lu, X.; Lan, T.; Qin, Z.; Wang, Z.; Zhou, G. *ACS Appl. Mater. Interfaces* **2014**, *6*, 19308. http://dx.doi.org/10.1021/am505153q
12. Kim, J-H.; Kim, H. U.; Song, C. E.; Park, M-J.; Kang, I-N.; Shin, W. S.; Hwang, D-H. *J. Polym. Sci. Pol. Chem.* **2013**, *51*, 2354. http://dx.doi.org/10.1002/pola.26614
13. Laursen, J. B.; Nielsen, J. *Chem. Rev.* **2004,** *104,* 1663. http://dx.doi.org/10.1021/cr020473j
14. Dsouza, R. N.; Pischel, U.; Nau, W. M. *Chem. Rev.* **2011**, *111*, 7941.

http://dx.doi.org/10.1021/cr200213s
15. Robins, K. A.; Jang, K.; Cao, B. Lee, D-C. *Phys. Chem. Chem. Phys.* **2010**, *12*, 12727. http://dx.doi.org/10.1039/c0cp00836b
16. Lee, D-C.; Cao, B.; Jang, K.; Forster, P. M. *J. Mater. Chem.* **2010**, *20*, 867. http://dx.doi.org/10.1039/B917601B
17. Mekler, V. M.; Bystryak, S. M. *Anal. Chim. Acta* **1992**, *264*, 359. http://dx.doi.org/10.1016/0003-2670(92)87025-G
18. Sylvestre, S.; Sebastian, S.; Oudayakumar, K.; Jayavarthanan, T.; Sundaraganesan, N. *Spectrochim. Acta A* **2012**, *96*, 401. http://dx.doi.org/10.1016/j.saa.2012.05.047
19. Hammett, L. P.; *J. Am. Chem. Soc*. **1937**, *59*, 96. http://dx.doi.org/10.1021/ja01280a022
20. Ryazanova, O. A.; Voloshin, I. M.; Makitruk, V. L.; Zozulya, V. N.; Karachevtsev, V. A. *Spectrochim. Acta A* **2007**, *66*, 849. http://dx.doi.org/10.1016/j.saa.2006.04.027
21. Matsui, M.; Suzuki, M.; Nunome, I.; Kubota, Y.; Funabiki, K.; Shiro, M.; Matsumoto, S.; Shiozaki, H. *Tetrahedron* **2008,** *64*, 8830, http://dx.doi.org/10.1016/j.tet.2008.06.079
22. Hansch, C.; Leo, A.;, Taft, R.W, *Chem. Rev*. **1991**, *97*, 165. http://dx.doi.org/10.1021/cr00002a004
23. Singh, P.; Baheti, A.; Thomas, K. R. J. *J. Org. Chem.* **2011**, *76*, 6134. http://dx.doi.org/10.1021/jo200857p
24. Cheng, J.; Wei, K.; Ma, X.; Zhou, X.; Xiang, H. *J. Phys. Chem. C* **2013**, *117*, 16552. http://dx.doi.org/10.1021/jp403750q
25. Udhayakumari, D.; Velmathi, S.; Sung, Y-M; Wu, S-P. *Sensors and Actuators B* **2014**, *198*, 285. http://dx.doi.org/10.1016/j.snb.2014.03.063
26. Wang, C.; Li, G.; Zhang, Q. *Tetrahedron Lett.* **2013**, *54*, 2633. http://dx.doi.org/10.1016/j.tetlet.2013.03.030
27. Gao, G-Y.; Qu, W-J.; Shi, B-B,; Zhang, P.; Lin, Q.; Yao, H.; Yang, W-L.; Zhang, Y-M.; Wei, T-B. *Spectrochim. Acta Part A: Molecular and Biomolecular Spectroscopy* **2014**, *121*, 514; http://dx.doi.org/10.1016/j.saa.2013.11.004
28. Shi, B-B.; Zhang, P.; Wei, T-B.; Yaoa, H.; Lina, Q.; Liua, J.; Zhang, Y-M. *Tetrahedron* **2013**, *69*, 7981. http://dx.doi.org/10.1016/j.tet.2013.07.007
29. Yang, L.; Li, X.; Yang, J.; Qu, Y.; Hua, J. *ACS Appl. Mater. Interfaces* **2013**, *5*, 1317. http://dx.doi.org/10.1021/am303152w
30. Biernat, K.; Malinowski, A.; Gnat, M. In *Biofuels - Economy, Environment and Sustainability*, Fang, Z. Eds.; InTech; **2013**, Chapter 5, 125.

http://dx.doi.org/10.5772/53831
31. Brownell, L. V.; Robins, K. A.; Jeong, Y.; Lee, Y.; Lee, D-C. *J. Phys. Chem. C* **2013**, *117*, 25236.
http://dx.doi.org/10.1021/jp407269p
32. Yella, A; Lee, H. W; Tsao, H. N.; Yi, C.; Chandiran, A. K.; Nazeeruddin, M. K.; Diau, E. W.; Yeh, C. Y.; Zakeeruddin, S. M.; Grätzel, M. *Science* **2011**, *334*, 629.
http://dx.doi.org/10.1126/science.1209688
33. Shi, J.; Chen, J.; Chai, Z.; Wang, H.; Tang, R.; Fan, K.; Wu, M.; Han, H.; Qin, J.; Peng, T.; Li, Q.; Li, Z. *J. Mater. Chem.* **2012**, *22*, 18830.
http://dx.doi.org/10.1039/c2jm33833e

Author Biography

Dr. Subhadeep Banerjee is an Assistant Professor at the Department of Chemistry, BITS-Pilani K.K. Birla Goa Campus, Goa, India since January 2013. Dr. Banerjee received his PhD in Chemistry from the University of Connecticut, USA in May 2011 and his MS in Chemistry from Cornell University, USA in May 2007. He did his B.Sc in chemistry with honors in 2001. He worked as a research scientist at Sigma-Aldrich Chemicals Pvt. Ltd. in Bangalore India from November 2011-November 2012, before joining his current assignment. His research fields of interest are synthesis of novel porphyrins with modulated optical properties and heteroacene based donor-acceptor molecules.

